

High Level *ab Initio* Study of Thermal 1,3-Sigmatropic Shift in $\text{CH}_2=\text{CHCH}_2\text{X}$ with $\text{X} = \text{BH}_2, \text{NH}_2,$ and CH_3

Jun Yong Choi, Chang Kon Kim, Chan Kyung Kim, and Ikchoon Lee*

Department of Chemistry, Inha University, Incheon 402-751, Korea

Received: March 5, 2002; In Final Form: April 10, 2002

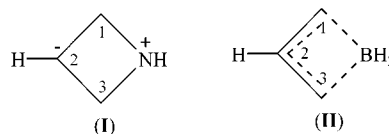
The thermal 1,3-sigmatropic migrations in $\text{X}-\text{CH}_2-\text{CH}=\text{CH}_2$ with $\text{X} = \text{BH}_2, \text{NH}_2,$ and CH_3 have been investigated at the RHF, MP2, B3LYP, G3, and CBS-APNO levels using basis sets with added diffuse and polarization functions. In all three cases, the suprafacial allowed path proceeds through a TS in which the $\text{C}=\text{C}$ π electron is delocalized into the 2p AO in the migrating X. For $\text{X} = \text{BH}_2$ with a vacant 2p orbital, the activation enthalpy is less than $1.0 \text{ kcal mol}^{-1}$ (CBS-APNO) so that the 1,3-shift is almost barrierless. For $\text{X} = \text{NH}_2$ there are two suprafacial pathways, one of which (higher energy path a) proceeds by participation of the lone pair on N. The lower energy pathway has a barrier height ($\Delta H^\ddagger = 68.9 \text{ kcal mol}^{-1}$) of only $1.0 \text{ kcal mol}^{-1}$ below the bond dissociation energy of the C^1-N bond, so that a diradical pathway can compete with the concerted sigmatropic shift. For $\text{X} = \text{CH}_3$, the activation barrier ($\Delta H^\ddagger = 76.1 \text{ kcal mol}^{-1}$) is higher (by ca. 1 kcal mol^{-1} at the CBS-APNO level) than the bond dissociation energy of the $\text{C}^1-\text{X}(\text{CH}_3)$ bond, so that the diradical reaction path is favored. The antarafacial 1,3-shifts are forbidden in all cases as evidenced by the second-order saddle-points (with two imaginary frequencies) and much higher barrier heights than those for the corresponding suprafacial shifts.

Introduction

The structure of the transition state (TS) and configuration of the product in the $[i,j]$ -sigmatropic rearrangement have been nicely predicted by the Woodward–Hoffmann selection rule using a simple orbital symmetry of the frontier molecular orbital approach.¹ For example, the rule predicts that thermal 1,3-sigmatropic rearrangement of hydrogen atom is allowed to take place via antarafacial TS but the 1,5-shift is forbidden.^{1,2} Also the rule predicts that both of the 1,3- and 1,5-sigmatropic shifts in which carbon is the migrating group are allowed to occur through the suprafacial TS but that thermal 1,3-migrations will proceed with inversion and thermal 1,5-migrations with retention of configuration within the migrating group.^{2,3} Many experimental results reported bear out the predictions of the simple rule.⁴

Although the orbital symmetry rule is very useful for the predictions of the TS structure and the product configuration in the sigmatropic rearrangements, there are some limitations. (i) In some cases, determination of the relevant frontier orbitals is ambiguous, e.g., if a migrating group has lone-pair electrons, it may become doubtful whether the lone-pair orbital is directly related as the frontier orbital or not. (ii) It is difficult to determine quantitatively the roles of migrating groups themselves influencing reactivities or TS structures. (iii) Although the sigmatropic rearrangements have been, in general, believed to occur via a single step concerted process, it is difficult to predict by using solely the orbital symmetry rule whether a sigmatropic rearrangement is really a concerted process or not. Indeed, Henriksen et al.⁵ have reported based on approximate *ab initio* PRDDO calculations⁶ that the 1,3-sigmatropic migration of allylamine occurs by a stepwise process through an intermediate of the nitrogen-containing four-membered cyclic structure with C_s

symmetry (I). Also, in the 1,3-shift of allylborane reported by Schleyer and co-workers,⁷ structure II is predicted to be a transition state with the barrier of $12.8 \text{ kcal mol}^{-1}$ at the HF/6-31G*//HF/6-31G* level. However, it is slightly more stable (by $0.6 \text{ kcal mol}^{-1}$) than the ground state at the MP2(full)/6-31G*//MP2(full)/6-31G* level. Therefore, the possibility that II is not a TS but is a minimum as suggested by Schleyer and co-workers⁷ cannot be entirely ruled out. If so, the 1,3-shift of allylborane may also be a stepwise process.



In this work, we have investigated theoretically thermal 1,3-sigmatropic migrations in $\text{X}-\text{CH}_2-\text{CH}=\text{CH}_2$, where $\text{X} = \text{BH}_2, \text{CH}_3$ and NH_2 , using high level *ab initio* MO and density functional theory (DFT) methods⁸ in order to examine closely the roles of migrating groups influencing reactivities or TS structures in the 1,3-sigmatropic shifts. In the three selected systems, the migrating group, X, bears lone pair electrons ($\text{X} = \text{NH}_2$), a vacant p-orbital ($\text{X} = \text{BH}_2$), or the saturated carbon atom ($\text{X} = \text{CH}_3$), and the factors affecting the migration are analyzed systematically as well as quantitatively.

Calculation

The Gaussian 98 program package⁹ with standard Pople-type basis sets¹⁰ was used throughout in this work. Geometries were optimized under the relevant symmetry constraints at the RHF, B3LYP,^{11,12} MP2, and QCISD¹³ levels of theory with various basis sets and the nature of each optimized structure being confirmed by frequency calculation¹⁴ at the theoretical levels employed, except for the QCISD/6-311+G** level for which

* To whom correspondence should be addressed. Fax: +82-32-865-4855. E-mail: ilee@inha.ac.kr.

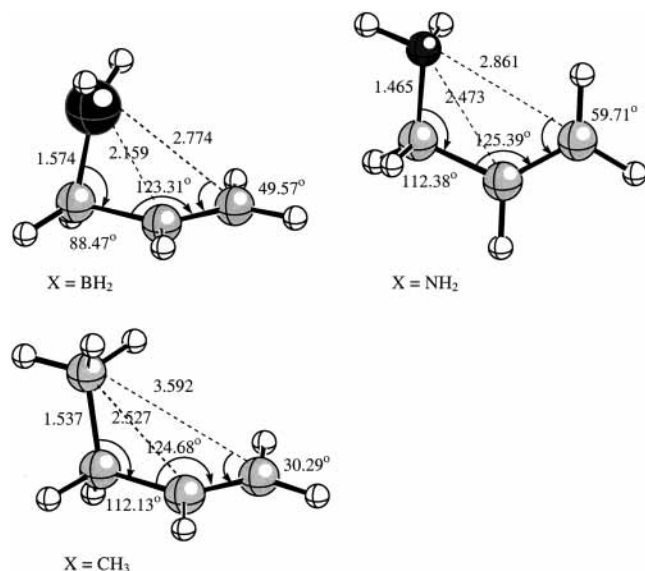


Figure 1. Optimized ground-state structures at the QCISD/6-311+G** level. Bond lengths are in Å, and bond angles are in degrees.

frequencies at the QCISD/6-31G* level were used. All antarafacial TSs with C_{2v} symmetry had two imaginary frequencies and hence are the second-order saddle points.¹⁵ The modified G3¹⁶ and CBS-APNO¹⁷ calculations were also carried out using the geometries optimized at the QCISD/6-311+G** level. The analyses such as charge densities and bond indices etc. were performed using the NBO-4M program¹⁸ interfaced to the Gaussian 98 program at the QCISD/6-311+G**/QCISD/6-311+G** level.

Results and Discussion

The ground-state structures optimized at the QCISD/6-311+G** level are shown in Figure 1. All have open geometries with unsymmetrical (C_1) structure. The empty p orbital on the boron atom in allylborane is directed toward the π orbital of the $C^2=C^3$ double bond. However, because of the repulsive interaction with the lone pair on the N atom, the $C^2=C^3$ π orbital in the allylamine is turned away from the molecular plane in order to alleviate direct n- π interaction. In 1-butene, the two hydrogen atoms on the terminal CH_3 group have a bifurcated arrangement to reduce steric repulsion. The ground-state energies calculated at various levels are summarized in Table S1 of the Supporting Information.

1,3-Sigmatropic Shift in Allylborane, $BH_2-CH_2-CH=CH_2$. It is appropriate here to discuss the MP2 results, which caused confusions in the past about the possibility of a stepwise process involving an intermediate (C_s) in the 1,3-shifts in allylborane.⁷ The optimized structures of the two stationary points along the suprafacial path with C_s and C_1 symmetries at the MP2/6-311++G** level are shown in Figure 2, and the energies calculated at the MP2 level using 3 different basis sets are collected in Table 1.

In all cases, the C_s structure has a lower energy ($\delta E = E(C_1) - E(C_s) > 0$) than the C_1 structure. Compared to the ground-state energies, the C_s level becomes lower as the larger basis sets are used $E(C_s) - E(GS) = +0.06, -0.02,$ and -0.13 kcal mol⁻¹ with 6-31+G*, 6-31++G**, and 6-311++G**, respectively. These MP2 results indicate that the C_s structure is an intermediate (with all real vibrational frequencies) and the C_1 structure is the TS (with only one imaginary frequency). However, the well depth corresponding to the energy difference between the two [$\delta E = E(C_1) - E(C_s)$] is very shallow

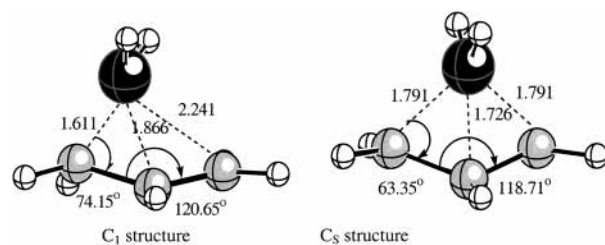


Figure 2. Optimized C_s and C_1 structures corresponding to the intermediate and TS, respectively, for the 1,3-shift of allylborane at the MP2/6-311++G** level. Bond lengths are in Å, and bond angles are in degrees.

TABLE 1: Calculated Electronic Energies of C_s (Intermediate) and C_1 Structures (TS) and the Energy Differences between the Two Structures for the BH_2 Shift in Allylborane at the MP2 Level

basis sets	E^a					
	C_s	C_1	δE^a	δE_{ZPE}^c	δH^d	δG^e
MP2/6-31+G*	-142.78497	-147.78453	+0.25	-0.04	-0.45	+0.38
MP2/6-31++G**	-142.84008	-142.83970	+0.25	-0.08	-0.50	+0.36
MP2/6-311++G**	-142.88268	-142.88234	+0.19	-0.22	-0.50	+0.31

^a Electronic energies in hartree. ^b Differences in electronic energies between C_s and C_1 structures, $\delta E = E(C_1) - E(C_s)$, in kcal mol⁻¹. ^c Differences in electronic energies corrected for zero-point vibration energies (ZPE) between C_s and C_1 structures, $\delta E_{ZPE} = E_{ZPE}(C_1) - E_{ZPE}(C_s)$, in kcal mol⁻¹. Corrected for zero-point vibration energies using the relevant scaling factors: Scott, A. P.; Radom, L. *J. Phys. Chem.* **1996**, *100*, 16502-16513. ^d Differences in enthalpies at 298 K between C_s and C_1 structures, $\delta H = H(C_1) - H(C_s)$, in kcal mol⁻¹. ^e Differences in the Gibbs free energies at 298 K between C_s and C_1 structures, $\delta G = G(C_1) - G(C_s)$, in kcal mol⁻¹.

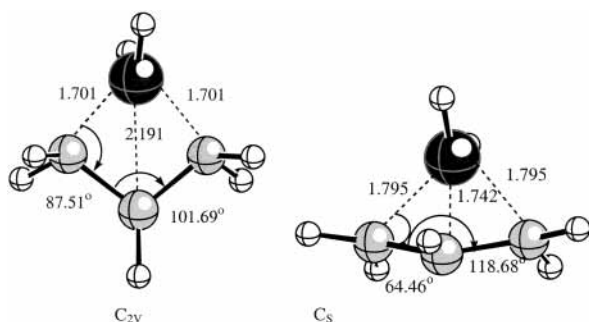
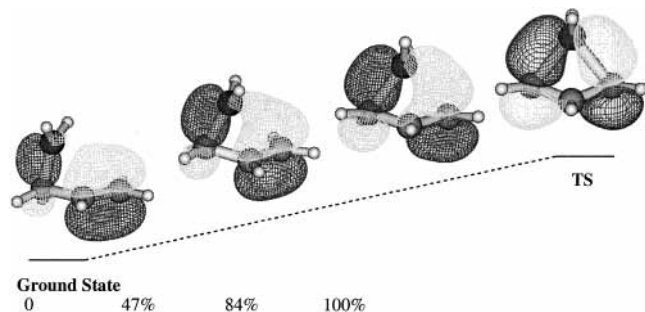
irrespective of the basis sets used (ca. 0.2 kcal mol⁻¹), so that the transition region is very flat. As a result, an inversion of the energy levels¹⁹ leading to an absurd result of a lower TS than the intermediate occurs when energies are corrected for zero-point energies ($\delta \Delta E_{ZPE}^\ddagger = \Delta E_{ZPE}^\ddagger(C_1) - \Delta E_{ZPE}^\ddagger(C_s) < 0$) and thermal energies ($\delta \Delta H^\ddagger = \Delta H^\ddagger(C_1) - \Delta H^\ddagger(C_s) < 0$). The level of the intermediate becomes higher than that of the TS because of the higher vibrational energy contribution to the intermediate than to the TS in the ΔE_{ZPE}^\ddagger and ΔH^\ddagger . The vibrational energy of the intermediate is higher than that of the TS mainly because an asymmetric stretching vibrational mode of the intermediate becomes a translational mode along the reaction coordinate in the TS and the vibrational contributions to the thermal energy and entropy of this vibrational mode are missing in the TS.¹⁹ The relative energy levels become restored to normal ($\delta G = G(C_1) - G(C_s) > 0$) only when the entropy effect is accounted for as can be seen in Table 1. In conclusion, the MP2 transition region for the 1,3-sigmatropic suprafacial (allowed) shift in allylborane with inversion of the migrating group ($X = BH_2$) configuration is very flat with an intermediate of the C_s symmetry which is marginally more stable (ca. 0.2 kcal mol⁻¹) than the TS of the C_1 symmetry. Thus, the MP2 results predict a stepwise migration of the BH_2 . This MP2 prediction is however in disagreement with the single step concerted shift involving the TS of C_s symmetry by all other methods listed in Table 2, i.e., RHF, B3LYP, QCISD, G3, and CBS-APNO. The suprafacial TS structure with C_s symmetry at the QCISD/6-311+G** level is shown in Figure 3.

Now, we may ask why the MP2 results alone make a wrong prediction? The answer to this lies in the overestimation of the electron correlation effect which results in the underestimation of the activation energy by the MP2 method for delocalized TS structures.²⁰ This is evident by considering the low MP2

TABLE 2: Calculated Activation Energies ($\Delta E_{\text{ZPE}}^\ddagger$)^a and Enthalpies (ΔH^\ddagger)^b for the Concerted Suprafacial and Antarafacial 1,3-Shift in Allylborane in kcal mol⁻¹

	levels	suprafacial		antarafacial	
		$\Delta E_{\text{ZPE}}^\ddagger$	ΔH^\ddagger	$\Delta E_{\text{ZPE}}^\ddagger$ ^a	ΔH^\ddagger ^b
RHF	6-31+G*	15.71	14.75	65.34	64.46
	6-31++G**	15.71	14.76	65.20	64.33
	6-311++G**	16.03	15.09	65.27	64.42
B3LYP	6-31+G*	3.25	2.55	55.75	55.27
	6-31++G**	3.15	2.44	55.03	54.56
	6-311++G**	3.72	3.00	55.17	54.68
QCISD	6-31G*	3.72	3.01	60.91	60.39
	6-311+G**	4.13	3.42	59.47	58.96
G3 ^(c)		2.23	1.52		
CBS-APNO ^(c)		1.16	0.46		

^a Corrected for zero-point vibration energies using the relevant scaling factors: Scott, A. P.; Radom, L. *J. Phys. Chem.* **1996**, *100*, 16502. ^b At 298 K. ^c Geometry obtained at the QCISD/6-311+G** level and zero-point vibration and thermal energies at the QCISD/6-31G* level were used.

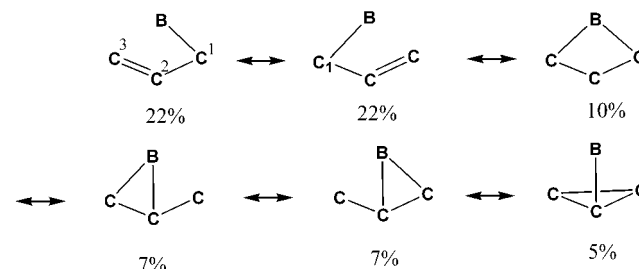
**Figure 3.** Optimized C_{2v} and C_s structures corresponding to the antarafacial and suprafacial TS, respectively, for the 1,3-shift in allylborane at the QCISD/6-311+G** level. Bond lengths are in Å, and bond angles are in degrees.**Figure 4.** Progressive variation of FMO shapes during the 1,3-shift of BH_2 in allylborane obtained by the IRC calculation at the B3LYP/6-31+G* level. The FMO shapes were drawn at the RHF/6-31+G**/B3LYP/6-31+G* level.

activation energies of $\Delta E^\ddagger \cong 0.2\sim 0.3$ kcal mol⁻¹ relative to all other correlated ΔE^\ddagger values of $2\sim 3$ kcal mol⁻¹. Progressive variation of the canonical frontier MO (CFMO) shape toward the suprafacial TS drawn at the RHF/6-31+G**/B3LYP/6-31+G* level is presented in Figure 4, where the $\text{C}^2=\text{C}^3$ π electron delocalization into the empty p orbital on the B atom can be clearly noted. Because the TS in this figure has a C_s structure (100% TS), the delocalization of π electron reaches to its maximum. In other words, in the C_1 structure, which should correspond to a point less than 100% TS (e.g., 84% TS) on the reaction coordinate, the delocalization of $\text{C}^2=\text{C}^3$ π electron should be less than that for the TS (C_s). As a result, the C_s structure will have larger electron correlation energy^{20b} (lower energy) than the C_1 structure by the MP2 method, albeit

TABLE 3: Charge Densities of the Migrating Groups, $q(X)$ in Electron Unit, Obtained at the NBO-QCISD/6-311+G** Level for the 1,3-Shifts

X	$q_0(X)$ ^a	$q^\ddagger(X)$ ^b	Δq^\ddagger
BH_2	+0.248 ^a	+0.001	-0.247
$\text{NH}_2(\text{a})$ ^d	-0.145	0.095	0.240
$\text{NH}_2(\text{b})$ ^e	-0.145	-0.233	-0.088
CH_3	+0.022	+0.006	-0.016

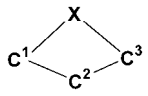
^a Charge densities at the ground state. ^b Charge densities at the TS. ^c $\Delta q^\ddagger = q^\ddagger(X) - q_0(X)$. ^d Path a. ^e Path b.

SCHEME 1

the energy difference due to the overestimated correlation energy may be small. This shows that for the very flat transition region the MP2 energetics may lead to a wrong prediction as to the nature of the TS, especially when a relatively strong delocalization structure is present near the true TS as evidenced by the prediction of an intermediate for the 1,3-shift in allylborane based on MP2 results by Schleyer and co-workers.⁷

The suprafacial 1,3-sigmatropic migration of BH_2 in allylborane takes place concertedly with inversion through the TS of C_s symmetry at all levels of calculation except for the MP2 level, and the activation energies and enthalpies are summarized in Table 2. We note that the account of the electron correlation effect results in substantial lowering of the $\Delta E_{\text{ZPE}}^\ddagger$ and ΔH^\ddagger values. The higher level, G3 and CBS-APNO, calculations lead to further depression of the barrier height, and indeed the best activation energy ($\Delta E_{\text{ZPE}}^\ddagger$) and enthalpy (ΔH^\ddagger) are a mere 1.2 and 0.5 kcal mol⁻¹, respectively. Thus, the 1,3-shift of BH_2 in allylborane should be very facile and proceed almost barrierlessly in the gas phase. It is noteworthy that the DFT (B3LYP) results are closer to the best values (CBS-APNO) than those at the QCISD level. Electron correlation energies for the TS (0.52294 hartree) and ground state (0.50931 hartree) calculated at the QCISD/6-31G* level indicate that the TS is stabilized by electron delocalization because of the $\pi_{\text{C}=\text{C}}-\text{p}_{\text{B}}^0$ charge-transfer interaction (the superscript zero stresses the empty character), because it is well-known that electron correlation enhances resonance delocalization.²² The charge density change on the migrating group, BH_2 , calculated by the natural population analysis (NPA)²³ in Table 3 indicates that the π -orbital charge is transferred to the vacant p orbital of boron increasing the negative charge ($\Delta q^\ddagger = q^\ddagger(X) - q_0(X) = -0.247$) in the TS. This charge shift can be confirmed by the progressive variation of frontier MO (FMO) shapes calculated at the RHF/6-31+G**/B3LYP/6-31+G* level on going from the ground state to the TS (Figure 4) along the (B3LYP/6-31+G*) intrinsic reaction coordinate (IRC).²⁴

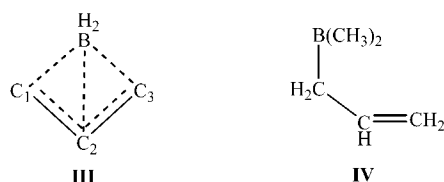
The strong resonance delocalization within the TS for the 1,3-shift in allylborane can also be shown by the natural resonance theory (NRT) analysis due to Weinhold and co-workers.²² The percentage weights (wt %) of resonance structures in the TS were calculated at the NBO-QCISD/6-311+G** level,²⁵ and the results are given in Scheme 1. The first three resonance structures correspond to the delocalized

TABLE 4: Natural Bond Order Analyses at the NBO-QCISD/6-311+G Level**


bond	BH ₂		NH ₂			CH ₃	
	GS	TS	GS	TS(a) ^a	TS(b) ^b	react	TS
C ¹ –C ²	1.908	1.291	1.953	1.071	1.510	1.952	1.527
C ² –C ³	1.026	1.291	1.057	1.071	1.510	1.028	1.527
C ³ –X	1.002	0.532	1.044	0.948	0.426	1.043	0.500
C ¹ –X	0	0.532	0	0.948	0.426	0	0.500
C ² –X	0.066	0.296	0	0.005	0	0	0
C ¹ –C ³	0	0.056	0	0	0	0	0

^a Path a. ^b Path b.

state **II**, whereas the last three correspond to the bicyclically delocalized structure **III**, with the transannular B–C² bond suggested by Henriksen et al.⁵ These NRT results are supported by the natural bond order (NBO) analysis²⁵ at the QCISD/6-311+G** level shown in Table 4. The bond order of 0.30 for the transannular B–C² bond is more than half as strong as those for the two bonds (0.53) between boron and the terminal carbon atoms, B–C¹ and B–C³.



It is clear that the strong resonance delocalization of the C=C π electrons to the empty p orbital of boron in the TS leads to a nearly barrierless 1,3-boron shift in the allylborane. For the 1,3-shift in dimethylallylborane, **IV**, the barrier observed experimentally²⁶ is reported to be ca. 10 kcal mol⁻¹ and theoretically at the MP2/6-31G**//6-31G* + ZPE level of 9.2 kcal mol⁻¹.⁷ This relatively higher barrier to the 1,3-shift in the dimethylallylborane, **IV**, than in the unsubstituted allylborane no doubt has steric and electronic origins. Sterically, there will be unfavorable steric interference of methyl groups with the allyl moiety, and electronically, the electron donating effect of the two methyl groups will raise the empty p orbital level of boron so that the π -p⁰ charge transfer will be less efficient due to the wider energy gap between π and p⁰ orbitals. These steric and electronic effects are further enhanced in the 1,3-shift of but-1-en-3-yl-(dimethylamino)ethylborane, for which the experimental barrier of 24.6 kcal mol⁻¹ has been reported.²⁷

The thermal concerted 1,3-shift with inversion of the migrating group, BH₂, is forbidden antarafacially.^{1,2} We have attempted to locate the antarafacial TS, but what we found was a C_{2v} structure corresponding to a second-order saddle point with two imaginary frequencies at all levels of theory employed in the present work (Table 2). The structure at the QCISD/6-311+G** level in Figure 3 shows that the angular distortion of the allyl group is much larger (decrease in $\angle C^1C^2C^3 \cong 22^\circ$) than that in the suprafacial TS (ca. 5°), albeit bond stretching is somewhat smaller ($\Delta d(C^1-B) = 0.127 \text{ \AA}$ vs 0.221 \AA). Overall, the C_{2v} structure for the antarafacial process is tighter than the C_s structure of the suprafacial TS. For this reason, the barrier height for the C_{2v} species is higher by more than 50 kcal mol⁻¹ than that of the C_s TS (Table 2).

1,3-Sigmatropic Shift in Allylamine, NH₂–CH₂–CH=CH₂. Allylamine has a lone-pair orbital (n_N) on the migrating

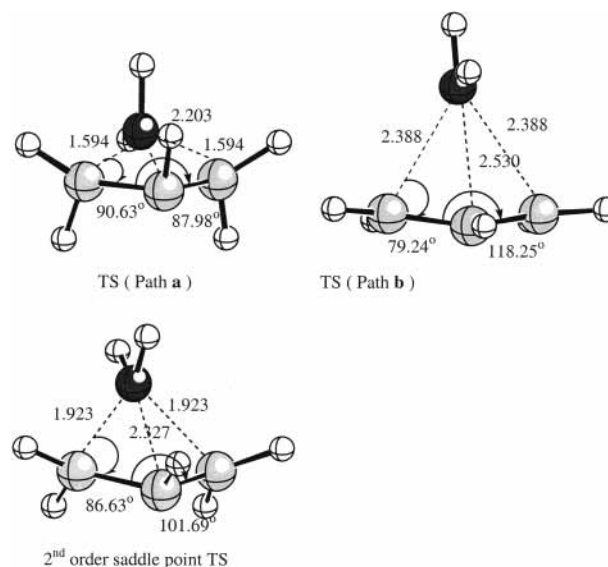


Figure 5. Optimized TS structures (paths a and b) and the second-order saddle point structure for the 1,3-shift in allylamine at the QCISD/6-311+G** level. Bond lengths are in \AA , and bond angles are in degrees.

group, X = NH₂, which is in contrast to an empty p orbital on X = BH₂ in allylborane discussed above. Henriksen et al.⁵ performed the PRDDO studies on the 1,3-shift in the allylamine and concluded that the migration of X = NH₂ takes place stepwise with a dipolar intermediate which is located lower by 4.7 kcal mol⁻¹ than the activation barrier of 98 kcal mol⁻¹. The very high barrier obtained was taken to reflect the difficulty to concerted rearrangement experienced by allylamine, although part of the barrier may be due to PRDDO's inflexible basis set and lack of diffuse orbitals for properly handling the carbanion center at C².⁵

This unusual, stepwise, mechanism predicted for the thermal 1,3-shift in allylamine by the PRDDO method⁶ prompted us to reexamine the mechanism using higher level correlated methods. The results are summarized in Table 5, where we note that there are two suprafacial 1,3-shift pathways (paths a and b). All correlated methods predict that path b has a lower energy barrier than path a, whereas the RHF (uncorrelated) method predicts the reverse ($\Delta H_b^\ddagger > \Delta H_a^\ddagger$). The TS structures in Figure 5 show that both the TSa and TSb have C_s symmetries and that the latter is much looser than the former. The progressive variation of FMO structure up to the TS for the path a in Figure 6 (TSa) reveals that the nitrogen lone pair forms the new bond to carbon (C³) making a four-membered cyclic structure, **I**. In the TS (not the intermediate as proposed by Henriksen et al.⁵), the electron density on N becomes deficient by $\Delta q = 0.240$ electron unit (Table 3) which accumulates on C² resulting in a dipolar structure. In contrast, the π electrons of the C²=C³ bond delocalize into the partially (half) filled 2p orbital of N, which is similar to the (C²=C³) π electron delocalization into the vacant 2p orbital of B in the 1,3-shift of allylborane discussed above. The difference between the two is that in the 1,3 shift of allylamine the partial N–C¹ bond dissociation should occur prior to, or concurrently with, the new N–C³ bond formation, whereas in the allylborane, no such bond cleavage is necessary (Figures 5 and 6). The stretching of the N–C¹ bond in the TSb is large with $\Delta d^\ddagger = 0.923 \text{ \AA}$ (compared to that in allylborane of $\Delta d^\ddagger = 0.221 \text{ \AA}$ and that in the TSa for allylamine of $\Delta d^\ddagger = 0.221 \text{ \AA}$). However, the angular distortion of the $\angle C^1C^2C^3$ in TSb is small (decrease of ca. 7°) compared to that in TSa (decrease of ca. 37°). Overall, the TSa is tightly bound, whereas

TABLE 5: Calculated Activation Energies ($\Delta E_{\text{ZPE}}^\ddagger$)^a and Enthalpies (ΔH^\ddagger)^b of Suprafacial and Antarafacial Paths for the 1,3-Shift in Allylamine and Bond Dissociation Enthalpy (ΔH_{BDE}) of N–C¹ Bond in kcal mol⁻¹

level		suprafacial								ΔH_{BDE}
		path (a)		path (b)		antarafacial		2nd order saddle point		
		$\Delta E_{\text{ZPE}}^\ddagger$	ΔH^\ddagger	$\Delta E_{\text{ZPE}}^\ddagger$	ΔH^\ddagger	$\Delta E_{\text{ZPE}}^\ddagger$	ΔH^\ddagger	$\Delta E_{\text{ZPE}}^\ddagger$	ΔH^\ddagger	
RHF	6-31+G*	86.78	86.15	93.49	93.29	93.52	92.55	94.33	93.75	
	6-31++G**	87.26	86.62	93.40	93.20	93.50	92.52	94.61	94.02	
	6-311++G**	87.22	86.45	94.00	93.68	93.33	92.21	95.20	94.48	
B3LYP	6-31+G*	73.29	72.82	69.69	69.56	83.34	82.36	73.20	72.57	
	6-31++G**	73.61	73.12	69.38	69.25	83.27	82.27	73.51	72.85	
	6-311++G**	74.78	74.32	69.31	69.20	84.11	83.12	74.51	73.86	
MP2	6-31+G*	75.59	75.04	71.87	71.65	87.12	86.10	75.62	74.92	
	6-31++G**	75.92	75.33	71.73	71.48	86.88	85.82	75.98	75.24	
	6-311++G**	75.05	74.42	72.22	72.01	85.27	84.23	75.81	75.11	
QCISD	6-31G*	81.33	80.79	76.93	76.89	91.46	90.47	81.87	81.22	
	6-311+G**	76.86	76.32	75.14	75.10	87.38	86.39	80.37	79.72	
G3 ^(c)		76.23	75.69	67.84	67.80					69.88
CBS-APNO ^(c)		75.39	74.85	68.94	68.90					70.18

^a Corrected for zero-point vibration energies using the relevant scaling factors: Scott, A. P.; Radom, L. *J. Phys. Chem.* **1996**, *100*, 16502. ^b At 298 K. ^c Geometry obtained at the QCISD/6-311+G** level and zero-point vibration and thermal energies at the QCISD/6-31G* level were used.

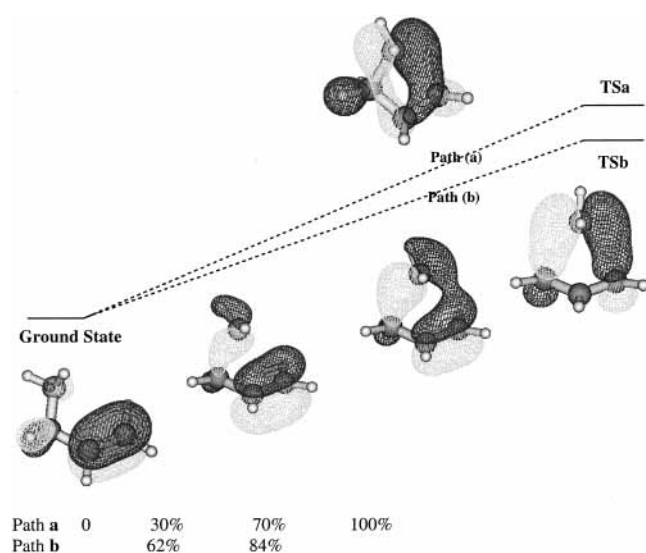


Figure 6. Progressive variation of FMO shapes during the 1,3-shift of NH₂ in allylamine obtained by the IRC calculation at the B3LYP/6-31+G* level. The FMO shapes were obtained at the RHF/6-31+G**//B3LYP/6-31+G* level.

the TSb is loose with rather strong electron delocalization. For example, the MP2 $\Delta E_{\text{ZPE}}^\ddagger$ value for path b with the 6-311++G** basis sets is lower by ca. 22 kcal mol⁻¹, but that for path a is only lower by ca. 12 kcal mol⁻¹ than the corresponding uncorrelated RHF values. Because electron correlation enhances charge delocalization,^{22b} the TSb has substantially greater delocalized structure. The best value (at the CBS-APNO level) for the enthalpy of activation (ΔH^\ddagger) is 68.9 kcal mol⁻¹ (compared with the PRDDO value of 98 kcal mol⁻¹) for path b which is lower by ca. 6 kcal mol⁻¹ than that for path a. Because the ΔH^\ddagger value is only lower by ca. 1 kcal mol⁻¹ than the C–N bond dissociation energy (BDE), the possibility of a diradical pathway cannot be entirely ruled out.²⁸

We have located another saddle point (C_s) corresponding to the antarafacial 1,3-shift of NH₂ in allylamine, which is second-order with two imaginary frequencies, between the two TSs, TSa and TSb, as shown in Figure 5 and Table 5. An extra imaginary frequency corresponds to the interconversion between the two TSs.

In summary, the 1,3-sigmatropic shift in allylamine proceeds by a concerted pathway (path b) which is quite similar to that

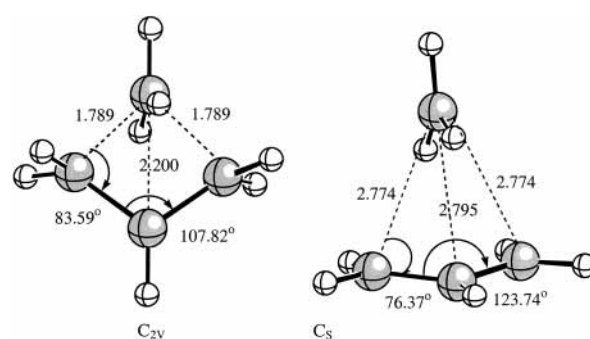


Figure 7. Optimized C_{2v} and C_s structures corresponding to the antarafacial and suprafacial TS, respectively, for the 1,3-shift in butene at the QCISD/6-311+G** level. Bond lengths are in Å, and bond angles are in degrees.

in allylborane. There is another pathway (path a) of higher barrier, in which the lone pair on N forms a new N–C³ bond, and a tight, dipolar TS (not an intermediate) is formed. All of the correlated MO results predict the lower barrier for path b, but it is reversed at the uncorrelated level (RHF). There is also a second-order saddle point corresponding to the antarafacial 1,3-shift of NH₂ in allylamine between the two TS (TSa and TSb). Because of the rather high activation barrier, which is lower only by ca. 1 kcal mol⁻¹ than the BDE (at the CBS-APNO level), a diradical pathway may be a possibility. The partial bond dissociation required in the TS (TSb) appears to cause the high barrier, and supports the possibility of a diradical pathway.

1,3-Sigmatropic Shift in 1-Butene, CH₃-CH₂-CH=CH₂. The two TS structures corresponding to the suprafacial (C_s) and antarafacial (C_{2v} symmetry second order saddle point with two imaginary frequencies) 1,3-shift of CH₃ in 1-butene at the QCISD/6-311+G** level are shown in Figure 7 and the energetics are summarized in Table 6. The progressive variation of the FMO shape from the ground state to the TS calculated at the RHF/6-31+G**//B3LYP/6-31+G* level along the IRC (B3LYP/6-31+G*) in Figure 8 indicates that here again the C=C π electrons are transferred to the half-filled 2p orbital of the migrating C atom. The loose TS structure with large C₁-X(CH₃) bond stretching ($\Delta d^\ddagger = 1.237$ Å) and small angular distortion (decrease in $\angle C^1C^2C^3 \cong 1^\circ$) leads to large activation enthalpy ($\Delta H^\ddagger = 76.1$ kcal mol⁻¹ at CBS-APNO level) for the allowed concerted CH₃ migration with inversion. The B3LYP results

TABLE 6: Calculated Activation Energies ($\Delta E_{\text{ZPE}}^\ddagger$)^a and Enthalpies (ΔH^\ddagger)^b of Suprafacial and Antarafacial Paths for the 1,3-shift in 1-butene and Bond Dissociation Enthalpy (ΔH_{BDE}) of the C¹-X(CH₃) Bond in kcal Mol⁻¹

level	suprafacial		antarfacial		ΔH_{BDE}
	$\Delta E_{\text{ZPE}}^\ddagger$	ΔH^\ddagger	$\Delta E_{\text{ZPE}}^\ddagger$	ΔH^\ddagger	
RHF	6-31+G*	108.75	105.78	195.51	194.87
	6-31++G**	107.27	104.33	192.55	192.10
	6-311++G**	106.84	103.78	190.54	190.11
B3LYP	6-31+G*	83.13	79.90	175.84	175.42
	6-31++G**	81.90	78.71	174.33	173.45
	6-311++G**	81.12	77.89	175.49	174.62
MP2	6-31+G*	86.23	82.21	178.03	177.11
	6-31++G**	85.18	81.38	175.30	174.39
	6-311++G**	84.10	80.27	169.35	168.44
QCISD	6-31G*	88.83	84.49	190.41	189.56
	6-311+G**	85.54	85.82	178.50	177.64
G3 ^(c)		73.93	74.24		74.08
CBS-APNO ^(c)		75.82	76.12		74.69

^a Corrected for zero-point vibration energies using the relevant scaling factors: Scott, A. P.; Radom, L. *J. Phys. Chem.* **1996**, *100*, 16502. ^b At 298 K. ^c Geometry obtained at the QCISD/6-311+G** level and zero-point vibration and thermal energies at the QCISD/6-31G* level were used.

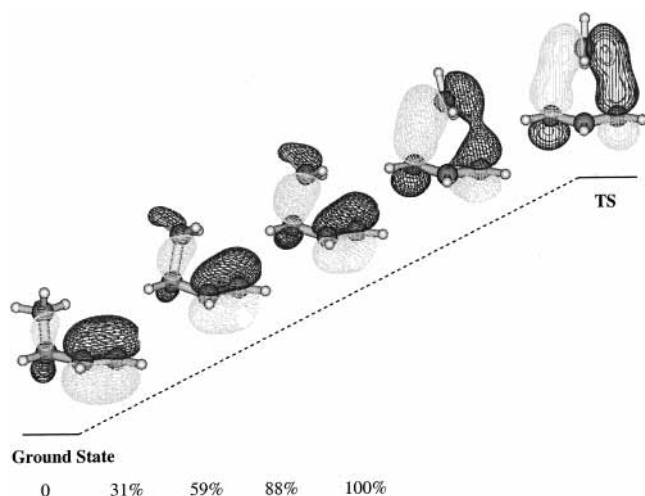


Figure 8. Progressive variation of FMO shape during the 1,3-shift of CH₃ in butene obtained by the IRC calculation at the B3LYP/6-31+G* level. The FMO shapes were obtained at the RHF/6-31+G*/B3LYP/6-31+G* level.

are closer to the best values at the CBS-APNO level than those at the MP2 and QCISD levels. The activation enthalpy of 76.1 kcal mol⁻¹ is, however, higher than the C¹-X(CH₃) bond dissociation energy (BDE = 74.7 kcal mol⁻¹) calculated at the same CBS-APNO level. This means that the loose suprafacial TS corresponds to the TS in a diradical pathway. This is reasonable because the large bond stretching of 1.237 Å at the TS should represent almost a dissociated state in which the carbon 2p orbital is half-filled with one electron. The C=C π electron flows into this half-filled 2p orbital as shown in Figure 8. The BDE of C¹-X(CH₃) is higher by 4 kcal mol⁻¹ than that of C¹-X(NH₂) at the CBS-APNO level. This is consistent with the experimental BDE difference between CH₃-CH₃ (97 kcal mol⁻¹) and CH₃-NH₂ (93 kcal mol⁻¹).²⁹ The resonance stabilized dissociated allylic radical (CH₂•-CH=CH₂) seems to lower the BDE of the C₁-X bonds uniformly in the two cases. The forbidden antarafacial shift is evident in an enormously high ΔH^\ddagger value (178 kcal mol⁻¹ at the QCISD level) in addition to the second-order nature of the C_{2v} saddle point. In summary, the suprafacial 1,3-shift of the diradical pathway

in which there is concurrent bond dissociation of the C¹-X(CH₃) bond and bond formation of the new C³-X(CH₃) bond occurs concertedly.

Acknowledgment. This work was supported by Korea Research Foundation for the 21st century.

Supporting Information Available: The ground-state energies calculated at various levels (Table S1). This material is available free of charge via the Internet at <http://pubs.acs.org>.

References and Notes

- (1) Woodward, R. B.; Hoffmann, R. *The Conservation of Orbital Symmetry*; Academic Press: New York, 1970; p 114.
- (2) Smith, M. B.; March, J. *March's Advanced Organic Chemistry*, 5th ed.; John Wiley & Sons: New York, 2001; p 1436.
- (3) Isaacs, N. *Physical Organic Chemistry*, 3rd Ed.; Longman Scientific & Technical: Harlow, U.K., 1995; p 748.
- (4) (a) Berson, J. A.; Nelson, G. L. *J. Am. Chem. Soc.* **1967**, *89*, 5503. (b) Berson, J. A. *Acc. Chem. Res.* **1968**, *1*, 152. (c) Boersma, M. A.; de Haan, J. W.; Kloosterziel, H.; van de Ven, L. J. M. *Chem. Commun.* **1970**, 1168. (d) Spangler, C. W. *Chem. Rev.* **1976**, *76*, 187. (e) Mironov, V. A.; Fedorovich, A. D.; Akhrem, A. A. *Russ. Chem. Rev.* **1981**, *50*, 666.
- (5) Henriksen, U.; Snyder, J. P.; Halgren, T. A. *J. Org. Chem.* **1981**, *46*, 3768.
- (6) (a) Halgren, T. A.; Lipscomb, W. N. *J. Chem. Phys.* **1973**, *58*, 1569. (b) Halgren, T. A.; Kleier, D. A.; Hall, J. H., Jr.; Brown, L. D.; Lipscomb, W. N. *J. Am. Chem. Soc.* **1978**, *100*, 6595.
- (7) Bühl, M.; Schleyer, P. v. R.; Ibrahim, M. A.; Clark, T. *J. Am. Chem. Soc.* **1991**, *113*, 2466.
- (8) (a) Hohenberg, P.; Kohn, W. *Phys. Rev. B* **1964**, *136*, 864. (b) Kohn, W.; Sham, L. J. *Phys. Rev. A* **1965**, *140*, 1133. (c) Salahub, D. R.; Zerner, M. C. Eds. *The Challenge of d and f Electrons*; American Chemical Society: Washington, DC, 1989. (d) Parr, D. R.; Yang, W. *Density-Functional Theory of Atoms and Molecules*; Oxford University Press: Oxford, U.K., 1989.
- (9) Frisch, M. J.; Trucks, G. W.; Schlegel, H. B.; Scuseria, G. E.; Robb, M. A.; Cheeseman, J. R.; Zakrzewski, V. G.; Montgomery, J. A., Jr.; Stratmann, R. E.; Burant, J. C.; Dapprich, S.; Millam, J. M.; Daniels, A. D.; Kudin, K. N.; Strain, M. C.; Farkas, O.; Tomasi, J.; Barone, V.; Cossi, M.; Cammi, R.; Mennucci, B.; Pomelli, C.; Adamo, C.; Clifford, S.; Ochterski, J.; Petersson, G. A.; Ayala, P. Y.; Cui, Q.; Morokuma, K.; Malick, D. K.; Rabuck, A. D.; Raghavachari, K.; Foresman, J. B.; Cioslowski, J.; Ortiz, J. V.; Stefanov, B. B.; Liu, G.; Liashenko, A.; Piskorz, P.; Komaromi, I.; Gomperts, R.; Martin, R. L.; Fox, D. J.; Keith, T.; Al-Laham, M. A.; Peng, C. Y.; Nanayakkara, A.; Gonzalez, C.; Challacombe, M.; Gill, P. M. W.; Johnson, B. G.; Chen, W.; Wong, M. W.; Andres, J. L.; Head-Gordon, M.; Replogle, E. S.; Pople, J. A. *Gaussian 98*, revision A.6; Gaussian, Inc.: Pittsburgh, PA, 1998.
- (10) Hehre, W. J.; Radom, L.; Schleyer, P. v. R.; Pople, J. A. *Ab Initio Molecular Orbital Theory*; John Wiley & Sons: New York, 1986; Chapter 4.
- (11) (a) Becke, A. D. *J. Chem. Phys.* **1993**, *98*, 5648. (b) Lee, C.; Yang, W.; Parr, R. G. *Phys. Rev. B* **1988**, *37*, 785. (c) Sosa, C.; Lee, C. *J. Chem. Phys.* **1993**, *98*, 8004.
- (12) Ricca, A.; Bauschlicher, C. W., Jr. *J. Phys. Chem.* **1995**, *99*, 9003.
- (13) Pople, J. A.; Head-Gordon, M.; Raghavachari, K. *J. Chem. Phys.* **1987**, *87*, 5968.
- (14) Ciszmadia, L. G. *Theory and Practice of MO Calculation on Organic Molecules*; Elsevier: Amsterdam, The Netherlands, 1976; p 239.
- (15) Schlegel, H. B. In *Encyclopedia of Computational Chemistry*; Schleyer, P. v. R., Ed.; John Wiley & Sons: New York, 1998; Vol. 2, p 1136.
- (16) (a) Baboul, A. G.; Curtiss, L. A.; Redfern, P. C.; Raghavachari, K. *J. Chem. Phys.* **1999**, *110*, 7650. (b) Curtiss, L. A.; Raghavachari, K.; Redfern, P. C.; Pople, J. A. *J. Chem. Phys.* **1998**, *109*, 7764.
- (17) Ochterski, J. W.; Petersson, G. A.; Montgomery, J. A. *J. Chem. Phys.* **1996**, *104*, 2598.
- (18) Glendening, E. D.; Badenhop, J. K.; Reed, A. E.; Carpenter, J. E.; Weinhold, F. *NBO 4.0*; Theoretical Chemistry Institute, University of Wisconsin: Madison, WI, 1999.
- (19) (a) Lee, I.; Kim, C. K.; Li, H. G.; Lee, B.-S.; Lee, H. W. *Chem. Phys. Lett.* **2000**, *320*, 307. (b) Kim, C. K.; Li, H. G.; Lee, H. W.; Sohn, C. K.; Chun, Y. I.; Lee, I. *J. Phys. Chem. A* **2000**, *104*, 4069.
- (20) (a) Raghavachari, K.; Whiteside, R. A.; Pople, J. A.; Schleyer, P. v. R. *J. Am. Chem. Soc.* **1981**, *103*, 5649. (b) Li, H. G.; Kim, C. K.; Lee, B.-S.; Kim, C. K.; Rhee, S. K.; Lee, I. *J. Am. Chem. Soc.* **2001**, *123*, 2326. (c) Kim, C. K.; Li, H. G.; Lee, B.-S.; Kim, C. K.; Lee, H. W.; Lee, I. *J. Org. Chem.* **2002**, *66*, 1593.

(21) Carsky, P.; Urban, M. *Ab Initio Calculations. Methods and Applications in Chemistry*; Springer-Verlag: Berlin, 1980; p 79.

(22) (a) Gonzales, C.; Schlegel, H. B. *J. Chem. Phys.* **1989**, *90*, 2154. (b) Gonzales, C.; Schlegel, H. B. *J. Phys. Chem.* **1990**, *94*, 5523. (c) Glendening, E. D.; Badenhop, J. K.; Weinhold, F. *J. Comput. Chem.* **1998**, *19*, 628 (d) Read, A. E.; Curtiss, L. A.; Weinhold, F. *Chem. Rev.* **1988**, *88*, 899. (e) Han, I. S.; Kim, C. K.; Lee, H. W.; Lee, I. J. *Phys. Chem. A* **2002**, *106*, 2554.

(23) (a) Reed, A. E.; Weinhold, F. *J. Chem. Phys.* **1983**, *78*, 4066. (b) Reed, A. E.; Weinstock, R. B.; Weinhold, F. *J. Chem. Phys.* **1985**, *83*, 735.

(24) (a) Glendening, E. D.; Weinhold, F. *J. Comput. Chem.* **1998**, *19*, 593. (b) Glendening, E. D.; Weinhold, F. *J. Comput. Chem.* **1998**, *19*, 610. (c) Glendening, E. D.; Badenhop, J. K.; Weinhold, F. *J. Comput. Chem.*

1998, *19*, 628.

(25) Foster, J. P.; Weinhold, F. *J. Am. Chem. Soc.* **1980**, *102*, 7211.

(26) Mikhailov, B. M. *Organomet. Chem. Rev., Sect. A* **1972**, *8*, 1.

(27) Hancock, K. G.; Kramer, J. D. *J. Am. Chem. Soc.* **1973**, *95*, 6463.

(28) (a) Newman-Evans, R. H.; Carpenter, B. K. *J. Am. Chem. Soc.* **1984**, *106*, 7994. (b) Pikulin, S.; Berson, J. A. *J. Am. Chem. Soc.* **1988**, *110*, 8500. (c) Klärner, F.; Yaslak, S.; Wette, M. *Chem. Ber.* **1979**, *112*, 1168. (d) Klärner, F.; Brassel, B. *J. Am. Chem. Soc.* **1980**, *102*, 2469. (e) Gajewski, J. J.; Gortva, A. M.; Bordon, J. E. *J. Am. Chem. Soc.* **1986**, *108*, 1083.

(29) Hehre, W. J.; Radom, L.; Schleyer, P. v. R.; Pople, J. A. *Ab Initio Molecular Orbital Theory*; John Wiley & Sons: New York, 1986; Chapter 4, p 278.